PERGAMON

International Journal of Solids and Structures 38 (2001) 7065–7078

INTERNATIONAL JOURNAL OF SOLIDS and STRUCTURES

www.elsevier.com/locate/ijsolstr

Multidomain boundary integral formulation for piezoelectric materials fracture mechanics

Giuseppe Davì *, Alberto Milazzo

Department of Mechanics and Aeronautics, University of Palermo, Viale delle Scienze, 90128 Palermo, Italy

Received 2 August 2000

Abstract

A boundary element method and its numerical implementation for the analysis of piezoelectric materials are presented with the aim to exploit their features in linear electroelastic fracture mechanics. The problem is formulated employing generalized displacements, that is displacements and electric potential, and generalized tractions, that is tractions and electric displacement. The generalized displacements boundary integral equation is obtained by using the closed form of the piezoelasticity fundamental solutions. These are derived through a displacement based modified Lekhnitskii's functions approach. The multidomain boundary element technique is implemented to achieve the numerical solution. Results are presented for typical fracture mechanics problems. The generalized stress intensity factors and the generalized relative crack displacements are computed to show the soundness of the approach. The results obtained are also analyzed to highlight some interesting features of the electroelastic coupling effects.

Keywords: Piezoelectric materials; Fracture mechanics; Boundary element method

1. Introduction

Piezoelectric materials generate an electric field when subjected to strain fields and undergo deformation when an electric field is applied. This inherent electromechanical coupling is widely exploited in the design of many devices working as transducers, sensors and actuators. In addition, piezoelectric materials are a primary concern in the field of advanced lightweight structures where the smart structure technology is now emerging (Crawley, 1987, 1994). By bonding or merging piezoelectric members within a structure it is possible to control the structure behavior through electrically induced strain fields and, conversely, employ the strain-induced electric field as a feedback driver. The effective control of piezoelectric smart structures can be achieved by means of the optimal combination of structural and control elements, which allows using all the benefits of the electromechanical coupling. This implies that the design of a piezoelectric smart structure refers to an accurate insight into the electromechanical response of the members of the structure.

* Corresponding author. Tel.: +390-91-665-7110; fax: +390-91-485-439.
E-mail address: davi@unipa.it (G. Davì).

0020-7683/01/$ - see front matter
PII: S0020-7683(00)00416-9

Analytical solutions to boundary value problems of piezoelectric solids are rather rare, due to the complexity of the governing equations. These solutions are for the most part devoted to interesting but simple problems of inclusions, inhomogeneities and dislocations (Pak, 1990b; Wang, 1992; Benveniste, 1992; Dunn, 1994a). To consider more realistic cases of technical interest numeric simulations need to be used. The first finite element solution for piezoelectric solids was proposed by Allik and Hughes (1970) and the method was applied successfully to general piezoelectric problems, as shown by the literature on the subject (Benjeddou, 2000). More recently the boundary element method (BEM) has been used to solve both two-dimensional (Lee and Jiang, 1994; Lee, 1995) and three-dimensional (Chen and Lin, 1995; Hill and Farris, 1998) piezoelectric problems. It was proved accurate and very efficient particularly when the investigation concerns two-dimensional piezoelastic bodies for which the fundamental solutions are known in closed form (Lee and Jiang, 1994; Lee, 1995; Sosa and Castro, 1990; Davì and Milazzo, 2000). A remarkable line of investigation involves crack problems in piezoelectric bodies (Parton, 1976). Indeed, due to the brittle behavior of piezoelectric materials, reliable service lifetime predictions demand a comprehensive understanding of the fracture process in the presence of electromechanical coupling. In this field analytical approaches have been developed for linear fracture mechanics and the relative solutions are based on eigenfunction expansion (Sosa and Pak, 1990), complex series expansion (Zhong and Meguid, 1997), superposition of distributed dislocations and electric dipoles (Pak, 1992), complex potentials (Pak, 1990a; Zhang and Tong, 1996) and complex variable approach (Suo et al., 1992; Park and Sun, 1995). Again, the analytical solutions above mentioned allow to analyze representative samples and numerical methods are required to approach the modelization and solution of piezoelasticity fracture mechanics complex problems. From this point of view, the BEM is particularly well suited and efficient to solve problems characterized by high stress gradients like crack problems (Aliabadi, 1997). The main advantages are the pointwise representation of the solution and the computational gain associated with the boundary discretization. Notwithstanding, there has been a certain lack of attention as regard the study of inclusion and crack problems in piezoelasticity by the integral equation approach. Only recently the BEM has been applied to piezoelastic fracture mechanics employing a single domain approach, which requires the use of hypersingular integral equations (Pan, 1999). In the present paper, piezoelastic fracture mechanics problems are investigated by using a multidomain boundary element approach (Davì and Milazzo, 2000). The formulation is based on the definition of the generalized displacements, that is mechanical displacements and electric potential. By using these generalized displacements one attains to a form of the governing equations that resembles the classic elasticity notation and it is very well suited to obtain the boundary integral representation. This representation for the generalized displacements is deduced starting from the piezoelasticity reciprocity theorem, which is the extension of the well-known elasticity reciprocity theorem to the electromechanical problem. The fundamental solutions, needed to infer the boundary integral representation, have been expressly determined by using a displacement based modified Lekhnitskii's functions approach (Lekhnitskii, 1963). The numerical solution of the formulation is obtained by BEM implementing its multidomain technique. Fracture mechanics analyses have been performed and the results obtained show the accuracy and robustness of the method. They also evidence interesting topics of the influence of the electromechanical coupling on the behavior of cracked piezoelectric solids.

2. Definitions and governing equations

Consider a transversely isotropic piezoelectric material and let it be referred to a co-ordinate system $x_1x_2x_3$, with the x_2 axis as the poling direction (Kiral and Eringen, 1990). Attention will be focused on two-dimensional problems for a body, which occupies the domain Ω, bounded by the contour $\partial\Omega$ in the x_1x_2 plane, so that the electromechanical response does not vary along the thickness direction x_3 (Pak, 1992). The piezoelastic analysis, corresponding to the arrangement of a generalized plane strain elasticity problem

and an in-plane electrostatic problem, involves the strains $\gamma = [\gamma_{11} \quad \gamma_{22} \quad \gamma_{33} \quad \gamma_{32} \quad \gamma_{31} \quad \gamma_{21}]^{\mathrm{T}}$, the stresses $\boldsymbol{\sigma} = [\sigma_{11} \quad \sigma_{22} \quad \sigma_{33} \quad \sigma_{32} \quad \sigma_{31} \quad \sigma_{21}]^{\mathrm{T}}$, the electric field $\mathbf{E} = [E_1 \quad E_2 \quad E_3]^{\mathrm{T}}$ and the electric displacement $\mathbf{D} = [D_1 \quad D_2 \quad D_3]^{\mathrm{T}}$. To obtain a compact and efficient matrix notation the strain γ_{33} and electric field component E_3, which are trivially zero due to the assumptions of generalized plane strain and in-plane electrostatics, are kept in the formulation. Let us introduce the mechanical displacement vector $\mathbf{u} = [u_1 \quad u_2 \quad u_3]^{\mathrm{T}}$ and the electric potential φ, which are functions of x_1 and x_2 only. The strain tensor and electric field vector are linked to mechanical displacements and electric potential by the compatibility equations

$$\boldsymbol{\gamma} = \mathscr{G}\mathbf{u} \tag{1}$$

$$\mathbf{E} = -\mathscr{L}\varphi \tag{2}$$

where

$$\mathscr{G} = \begin{bmatrix} \partial/\partial x_1 & 0 & 0 & 0 & 0 & \partial/\partial x_2 \\ 0 & \partial/\partial x_2 & 0 & 0 & 0 & \partial/\partial x_1 \\ 0 & 0 & 0 & \partial/\partial x_2 & \partial/\partial x_1 & 0 \end{bmatrix}^{\mathrm{T}} \tag{3}$$

$$\mathscr{L} = [\partial/\partial x_1 \quad \partial/\partial x_2 \quad 0]^{\mathrm{T}} \tag{4}$$

The following relations give the elasticity and electrostatics governing equations

$$\mathscr{G}^{\mathrm{T}}\boldsymbol{\sigma} + \mathbf{f} = \mathbf{0} \tag{5}$$

$$\mathscr{L}^{\mathrm{T}}\mathbf{D} - q = 0 \tag{6}$$

which are the equilibrium equations and the Gauss' s law for electrostatics, respectively. In Eqs. (5) and (6), $\mathbf{f} = [f_1 \quad f_2 \quad f_3]^{\mathrm{T}}$ and q are the body force vector and the electric charge density, respectively. Finally, the constitutive equations for transversely isotropic piezoelectric materials assume the following form

$$\begin{bmatrix} \boldsymbol{\sigma} \\ \mathbf{D} \end{bmatrix} = \begin{bmatrix} \sigma_{11} \\ \sigma_{22} \\ \sigma_{33} \\ \sigma_{32} \\ \sigma_{31} \\ \sigma_{21} \\ D_1 \\ D_2 \\ D_3 \end{bmatrix} = \begin{bmatrix} C_{11} & C_{12} & C_{13} & 0 & 0 & 0 & 0 & -e_{21} & 0 \\ C_{12} & C_{22} & C_{12} & 0 & 0 & 0 & 0 & -e_{22} & 0 \\ C_{13} & C_{12} & C_{11} & 0 & 0 & 0 & 0 & -e_{21} & 0 \\ 0 & 0 & 0 & C_{44} & 0 & 0 & 0 & 0 & -e_{14} \\ 0 & 0 & 0 & 0 & \frac{1}{2}(C_{11} - C_{13}) & 0 & 0 & 0 & 0 \\ 0 & 0 & 0 & 0 & 0 & C_{44} & -e_{14} & 0 & 0 \\ 0 & 0 & 0 & 0 & 0 & e_{14} & \varepsilon_{11} & 0 & 0 \\ e_{21} & e_{22} & e_{21} & 0 & 0 & 0 & 0 & \varepsilon_{22} & 0 \\ 0 & 0 & 0 & e_{14} & 0 & 0 & 0 & 0 & \varepsilon_{11} \end{bmatrix} \begin{bmatrix} \gamma_{11} \\ \gamma_{22} \\ \gamma_{33} \\ \gamma_{32} \\ \gamma_{31} \\ \gamma_{21} \\ E_1 \\ E_2 \\ E_3 \end{bmatrix}$$
$$= \begin{bmatrix} \mathbf{C} & -\mathbf{e}^{\mathrm{T}} \\ \mathbf{e} & \boldsymbol{\varepsilon} \end{bmatrix} \begin{bmatrix} \boldsymbol{\gamma} \\ \mathbf{E} \end{bmatrix} \tag{7}$$

where C_{ij} are the elastic coefficients, measured in a constant electric field, e_{ij} are the piezoelectric constants and ε_{ij} are the dielectric constants, measured at constant strain. According to Barnett and Lothe (1975), it is possible to introduce suitable electroelastic quantities given by the generalized displacements $\mathbf{U}$, the generalized body forces $\mathbf{F}$ and the generalized strains and stresses $\boldsymbol{\Gamma}$ and $\boldsymbol{\Sigma}$, which are defined as follows

$$\mathbf{U} = [u_1 \quad u_2 \quad u_3 \quad \varphi]^{\mathrm{T}} \tag{8}$$

$$\mathbf{F} = [f_1 \quad f_2 \quad f_3 \quad -q]^{\mathrm{T}} \tag{9}$$

$$\boldsymbol{\Gamma} = [\,\gamma_{11} \quad \gamma_{22} \quad \gamma_{33} \quad \gamma_{32} \quad \gamma_{31} \quad \gamma_{21} \quad -E_1 \quad -E_2 \quad -E_3\,]^{\mathrm{T}} \tag{10}$$

$$\boldsymbol{\Sigma} = [\,\sigma_{11} \quad \sigma_{22} \quad \sigma_{33} \quad \sigma_{32} \quad \sigma_{31} \quad \sigma_{21} \quad D_1 \quad D_2 \quad D_3\,]^{\mathrm{T}} \tag{11}$$

By introducing the differential operator

$$\mathscr{D} = \begin{bmatrix} \mathscr{G} & \mathbf{0} \\ \mathbf{0} & \mathscr{L} \end{bmatrix} \tag{12}$$

and the generalized stiffness matrix

$$\mathbf{R} = \begin{bmatrix} \mathbf{C} & \mathbf{e}^{\mathrm{T}} \\ \mathbf{e} & -\boldsymbol{\varepsilon} \end{bmatrix} \tag{13}$$

the governing equations of the problem, i.e. Eqs. (1)–(7), can be recast as

$$\boldsymbol{\Gamma} = \mathscr{D}\mathbf{U} \tag{14}$$

$$\boldsymbol{\Sigma} = \mathbf{R}\boldsymbol{\Gamma} \tag{15}$$

$$\mathscr{D}^{\mathrm{T}}\boldsymbol{\Sigma} + \mathbf{F} = \mathbf{0} \tag{16}$$

By combining Eqs. (14), (15) and (16), one obtains the governing equations of the piezoelastic problem in terms of generalized displacements

$$\mathscr{D}^{\mathrm{T}}\mathbf{R}\mathscr{D}\mathbf{U} + \mathbf{F} = \mathbf{0} \tag{17}$$

The boundary conditions on the restrained boundary $\partial\Omega_1$ are given in terms of prescribed generalized displacements

$$\mathbf{U} = \overline{\mathbf{U}} \quad \text{on } \partial\Omega_1 \tag{18}$$

whereas on the free boundary $\partial\Omega_2$ they are given in terms of prescribed generalized tractions (Suo et al., 1992)

$$\mathbf{T} = \overline{\mathbf{T}} \quad \text{on } \partial\Omega_2 \tag{19}$$

The generalized tractions $\mathbf{T}$, i.e. mechanical tractions and the normal component of the electric displacement, are defined by the following relation

$$\mathbf{T} = \begin{bmatrix} t_1 \\ t_2 \\ t_3 \\ D_n \end{bmatrix} = \mathscr{D}_n^{\mathrm{T}}\mathbf{R}\mathscr{D}\mathbf{U} \tag{20}$$

In the above equation $\mathscr{D}_n$ is the generalized traction operator, obtained from the differential operator $\mathscr{D}$ by replacing the derivatives with the corresponding direction cosines of the boundary outer normal (Davì and Milazzo, 1997).

3. Boundary integral representation

Let $\mathbf{U}_j$ be the generalized displacements which characterize a fictitious solution of the piezoelastic problem and that satisfies the equilibrium equation for given generalized body forces $\mathbf{F}_j$

$$\mathscr{D}^{\mathrm{T}}\mathbf{R}\mathscr{D}\mathbf{U}_j + \mathbf{F}_j = \mathbf{0} \tag{21}$$

Let $\boldsymbol{\Sigma}_j$ and $\boldsymbol{\Gamma}_j$ denote the generalized stress and strain fields, associated with $\mathbf{U}_j$, whereas $\mathbf{T}_j$ are the related generalized tractions. Taking the nature of Eq. (17) into consideration, the following reciprocity theorem holds for the actual piezoelastic response and the above-introduced fictitious solution (Davì and Milazzo, 2000)

$$\int_{\partial\Omega}\left(\mathbf{U}_j^{\mathrm{T}}\mathbf{T}-\mathbf{T}_j^{\mathrm{T}}\mathbf{U}\right)\mathrm{d}\,\partial\Omega=\int_{\Omega}\left(\mathbf{F}_j^{\mathrm{T}}\mathbf{U}-\mathbf{U}_j^{\mathrm{T}}\mathbf{F}\right)\mathrm{d}\Omega \tag{22}$$

Eq. (22) is the extension of the classic Betti's reciprocity theorem to the electroelastic problem. It represents the starting point to deduce the boundary integral representation for piezoelasticity. Consider $\mathbf{U}_j$ as a particular fictitious solution associated with a system of concentrated generalized body forces $\mathbf{F}_j$, applied at the point P_0

$$\mathbf{F}_j=\mathbf{c}_j\delta(P-P_0) \tag{23}$$

where $\mathbf{c}_j$ is the load intensity and $\delta(P-P_0)$ indicates the Dirac's function. For this selection of the particular solution, known as the fundamental solution of the problem, the reciprocity theorem provides the following relationship

$$\mathbf{c}_j^{\mathrm{T}}\mathbf{U}(P_0)+\int_{\partial\Omega}\left(\mathbf{T}_j^{\mathrm{T}}\mathbf{U}-\mathbf{U}_j^{\mathrm{T}}\mathbf{T}\right)\mathrm{d}\,\partial\Omega=\int_{\Omega}\mathbf{U}_j^{\mathrm{T}}\mathbf{F}\,\mathrm{d}\Omega \tag{24}$$

Eq. (24) is the electroelastic boundary integral representation and it is the analogous of the Somigliana identity of the elasticity extended to the electromechanical problem (Lee and Jiang, 1994; Davì and Milazzo, 2000). By using four independent fundamental solutions ($j=1,\ldots,4$), associated with concentrated forces directed along the axes and to a concentrated charge, one obtains the three displacement components and the electric potential at the point P_0 in terms of the displacements, tractions, electric potential and normal electric displacement on the boundary of the body. In matrix form, the boundary integral representation is given by

$$\mathbf{c}^*\mathbf{U}(P_0)+\int_{\partial\Omega}(\mathbf{T}^*\mathbf{U}-\mathbf{U}^*\mathbf{T})\mathrm{d}\,\partial\Omega=\int_{\Omega}\mathbf{U}^*\mathbf{F}\,\mathrm{d}\Omega \tag{25}$$

The kernels $\mathbf{U}^*$ and $\mathbf{T}^*$, appearing in Eq. (25), are defined as

$$\mathbf{U}^*=\left[U_{ij}\right]^{\mathrm{T}} \tag{26}$$

$$\mathbf{T}^*=\left[T_{ij}\right]^{\mathrm{T}} \tag{27}$$

where U_{ij} and T_{ij} indicate the ith component of the generalized displacements and tractions of the jth fundamental solution. The matrix $\mathbf{c}^*$ is defined by (Davì, 1989)

$$\mathbf{c}^*=-\int_{\partial\Omega}\mathbf{T}^*\mathrm{d}\,\partial\Omega \tag{28}$$

For P_0 belonging to the boundary $\partial\Omega$, Eq. (25) provides the boundary integral equations, which link the variables on the boundary. The boundary integral equations, coupled with the appropriate boundary conditions, allow determining the unknowns on the boundary. Once the boundary solution is determined, Eq. (25) gives the generalized displacements at the laminate generic internal point P_0. The generalized strains at P_0 can be calculated in a pointwise fashion by pre-multiplying Eq. (25) by $\mathbf{c}^{*-1}$ and then differentiating with respect to the source point P_0. One deduces the following boundary integral representation for the generalized strain field (Banerjee and Butterfield, 1981)

$$\boldsymbol{\Gamma}(P_0) = \int_{\partial\Omega} (\boldsymbol{\Xi}^*\mathbf{T} - \boldsymbol{\Theta}^*\mathbf{U})\mathrm{d}\,\partial\Omega + \int_{\Omega} \boldsymbol{\Xi}^*\mathbf{F}\,\mathrm{d}\Omega \tag{29}$$

where

$$\boldsymbol{\Theta}^* = -\mathscr{D}\mathbf{c}^{*-1}\mathbf{T}^* \tag{30}$$

$$\boldsymbol{\Xi}^* = -\mathscr{D}\mathbf{c}^{*-1}\mathbf{U}^* \tag{31}$$

Finally, the boundary integral representation for the generalized stresses can be simply obtained by pre-multiplying Eq. (29) for the extended stiffness matrix $\mathbf{R}$. One has

$$\boldsymbol{\Sigma}(P_0) = \int_{\partial\Omega} (\mathbf{R}\boldsymbol{\Xi}^*\mathbf{T} - \mathbf{R}\boldsymbol{\Theta}^*\mathbf{U})\mathrm{d}\,\partial\Omega + \int_{\Omega} \mathbf{R}\boldsymbol{\Xi}^*\mathbf{F}\,\mathrm{d}\Omega \tag{32}$$

4. Fundamental solutions

The formulation of the boundary integral equations needs the knowledge of an electroelastic solution of the piezoelectric domain loaded by concentrated generalized body forces applied at the point P_0. The fundamental solution is therefore governed in the domain Ω by the following equilibrium equation

$$\mathscr{D}^{\mathrm{T}}\mathbf{R}\mathscr{D}\mathbf{U}_j + \mathbf{c}_j\delta(P - P_0) = \mathbf{0} \tag{33}$$

A particular solution of Eq. (33) has been deduced by Lee and Jiang (1994), who employed the double Fourier transform method. Sosa and Castro (1994) obtained the fundamental solution through a state space approach coupled with the Fourier analysis. More recently, Pan (1999) proposed an approach based on the complex variable functions to determine the Green's functions for piezoelectric solids. In the present paper the fundamental solution is directly deduced by a variant of the Lekhnitskii's functions method (Lekhnitskii, 1963). The stress functions approach, employed for anisotropic elasticity by Lekhnitskii, is here extended to piezoelasticity and reformulated in terms of generalized displacements. Observing that Eq. (33) is a homogeneous equation (Lekhnitskii, 1963), except that at the point P_0 where the solution is singular, it admits particular solutions of the form

$$\mathbf{U} = \lambda\mathbf{a}\,\ln\,(X_1 + \mu X_2) \tag{34}$$

where $\mathbf{a}$, μ and λ are complex constants to be determined and

$$X_i = x_i(P) - x_i(P_0) \quad (i = 1, 2) \tag{35}$$

Substitution of Eq. (34) into Eq. (33) leads to the eigenvalue problem corresponding to Eq. (33), that is

$$\left[\mathbf{I}_1^{\mathrm{T}}\mathbf{R}\mathbf{I}_1 + \mu\left(\mathbf{I}_1^{\mathrm{T}}\mathbf{R}\mathbf{I}_2 + \mathbf{I}_2^{\mathrm{T}}\mathbf{R}\mathbf{I}_1\right) + \mu^2\mathbf{I}_2^{\mathrm{T}}\mathbf{R}\mathbf{I}_2\right]\mathbf{a} = \mathbf{0} \tag{36}$$

where the matrix $\mathbf{I}_m$ $(m = 1, 2)$ is obtained from the operator $\mathscr{D}$ by setting the derivative with respect to x_m equal to one and replacing all the other terms with zeros. The solution of Eq. (36) gives eight eigenvalues μ_k and the relative eigenvectors $\mathbf{a}_k$, which form conjugate pairs for stable materials. The fundamental solutions are obtained by superposing eight solutions of the form (34), associated with the eight eigenvalues μ_k. If $\mathrm{Im}(\mu_k) > 0$, the generalized displacements $\mathbf{U}_j$ of the fundamental solution are given by

$$\mathbf{U}_j = 2\sum_{k=1}^{4}\mathrm{Re}\left[\lambda_{kj}\mathbf{a}_k\,\ln\,(X_1 + \mu_k X_2)\right] \tag{37}$$

The generalized tractions are obtained from the following relation

$$\mathbf{T}_j = 2\sum_{k=1}^{4}\mathrm{Re}\left[\lambda_{kj}\mathscr{D}_n^{\mathrm{T}}\mathbf{R}\mathscr{D}_{\mu_k}\mathbf{a}_k\frac{1}{X_1+\mu_k X_2}\right] \tag{38}$$

where the matrix $\mathscr{D}_{\mu_k}$ is obtained from the operator $\mathscr{D}$ by replacing the derivative with respect to x_1 with one and the derivative with respect to x_2 with μ_k. The constants λ_{kj} are determined by enforcing the compatibility and equilibrium conditions. The vector $\boldsymbol{\lambda}_j = [\,\lambda_{1j} \quad \lambda_{2j} \quad \lambda_{3j} \quad \lambda_{4j}\,]^{\mathrm{T}}$ is then computed by

$$\boldsymbol{\lambda}_j = (\mathbf{B} + \tilde{\mathbf{B}}\tilde{\mathbf{A}}^{-1}\mathbf{A})^{-1}\mathbf{c}_j \tag{39}$$

where the tilde denotes the complex conjugate, $\mathbf{A}$ is the eigenvectors matrix and the columns $\mathbf{b}_k$ of the matrix $\mathbf{B}$ are defined as

$$\mathbf{b}_k = \overline{\mathscr{D}}_k\mathbf{R}\mathscr{D}_{\mu_k}\mathbf{a}_k \tag{40}$$

where

$$\overline{\mathscr{D}}_k = \pi\frac{1+\sqrt{-1}\mu_k}{1+\mu_k^2}\begin{bmatrix} -1 & 0 & 0 & 0 & 0 & \sqrt{-1} & 0 & 0 & 0 \\ 0 & \sqrt{-1} & 0 & 0 & 0 & -1 & 0 & 0 & 0 \\ 0 & 0 & 0 & \sqrt{-1} & -1 & 0 & 0 & 0 & 0 \\ 0 & 0 & 0 & 0 & 0 & 0 & -1 & \sqrt{-1} & 0 \end{bmatrix} \tag{41}$$

It is worth noting that the present fundamental solution has been derived by using a suitable matrix notation, which is very advantageous for computer implementation.

5. Numerical model and solution

The boundary integral equation formulation is solved numerically by the BEM (Banerjee and Butterfield, 1981). The boundary $\partial\Omega$ is discretized into m boundary elements and over each of these elements $\partial\Omega_{\langle k\rangle}$ the generalized displacements and tractions, $\mathbf{U}$ and $\mathbf{T}$, are expressed in terms of their respective nodal values $\boldsymbol{\Delta}_{\langle k\rangle}$ and $\mathbf{P}_{\langle k\rangle}$

$$\mathbf{U} = \mathbf{N}\boldsymbol{\Delta}_{\langle k\rangle} \quad \text{on } \partial\Omega_{\langle k\rangle} \tag{42}$$

$$\mathbf{T} = \boldsymbol{\Psi}\mathbf{P}_{\langle k\rangle} \quad \text{on } \partial\Omega_{\langle k\rangle} \tag{43}$$

where $\mathbf{N}$ and $\boldsymbol{\Psi}$ are matrices of standard shape functions whose order depends on the class of boundary elements used in the numerical model. In the absence of generalized body forces, the discretized version of Eq. (25) for any point P_i is therefore given by

$$\mathbf{c}_i^*\mathbf{U}(P_i) + \sum_{k=1}^{m}\mathbf{H}_{ik}\boldsymbol{\Delta}_{\langle k\rangle} + \sum_{k=1}^{m}\mathbf{G}_{ik}\mathbf{P}_{\langle k\rangle} = \mathbf{0} \tag{44}$$

where

$$\mathbf{H}_{ik} = \int_{\partial\Omega_{\langle k\rangle}}\mathbf{T}^*(P,P_i)\mathbf{N}(P)\,\mathrm{d}\,\partial\Omega \tag{45}$$

$$\mathbf{G}_{ik} = -\int_{\partial\Omega_{\langle k\rangle}}\mathbf{U}^*(P,P_i)\boldsymbol{\Psi}(P)\,\mathrm{d}\,\partial\Omega \tag{46}$$

By taking the field point P_i to all boundary nodes using a collocation technique and absorbing the $\mathbf{c}_i^*$ matrix with the corresponding block of $\mathbf{H}_{ii}$, one obtains a linear algebraic system, which can be compactly written as (Banerjee and Butterfield, 1981)

$$\mathbf{H}\boldsymbol{\Delta} - \mathbf{G}\mathbf{P} = \mathbf{0} \tag{47}$$

where $\mathbf{H}$ and $\mathbf{G}$ are the square influence matrices, $\boldsymbol{\Delta}$ is the vector of the nodal values of the generalized displacements and $\mathbf{P}$ the vector of the nodal values of the generalized tractions, respectively. Eq. (47), coupled with the electromechanical boundary conditions, provides the solution of the problem. If the investigated domain is made up of piece-wise different materials the problem can be solved by the multidomain BEM (Banerjee and Butterfield, 1981; Blandford et al., 1981; Tan et al., 1992). This approach is based on the division of the original domain into homogeneous subregions so that Eqs. (44) and (47) still hold for each single subdomain and one can write

$$\mathbf{H}^{(i)}\boldsymbol{\Delta}^{(i)} - \mathbf{G}^{(i)}\mathbf{P}^{(i)} = \mathbf{0} \quad (i = 1, 2 \ldots M) \tag{48}$$

where M is the number of subregions considered and the superscript (i) indicates quantities associated with the ith subdomain. To obtain the solution one has to restore the domain unity by enforcing the generalized displacement and traction continuity conditions along the interfaces between contiguous subdomains. Let us introduce a partition of the linear algebraic system given by Eq. (48) in such a way that the generic vector $\boldsymbol{y}^{(i)}$ can be written as

$$\boldsymbol{y}^{(i)} = \begin{bmatrix} \boldsymbol{y}^{(i)}_{\partial\Omega_{i1}} \\ \vdots \\ \boldsymbol{y}^{(i)}_{\partial\Omega_{iM}} \end{bmatrix} \tag{49}$$

In Eq. (49) the vector $\boldsymbol{y}^{(i)}_{\partial\Omega_{ij}}$ collects the components of $\boldsymbol{y}^{(i)}$ associated with the nodes belonging to the interface $\partial\Omega_{ij}$ between the ith and jth subdomain, with the convention that $\partial\Omega_{ii}$ denotes the external boundary of the ith subdomain (see Fig. 1). By so doing in the discretized model the interface compatibility and equilibrium conditions, that is the interface continuity conditions, are given by

$$\boldsymbol{\Delta}^{(i)}_{\partial\Omega_{ij}} = \boldsymbol{\Delta}^{(j)}_{\partial\Omega_{ij}} \quad (i = 1 \ldots M-1;\ j = i+1 \ldots M) \tag{50}$$

$$\mathbf{P}^{(i)}_{\partial\Omega_{ij}} = -\mathbf{P}^{(j)}_{\partial\Omega_{ij}} \quad (i = 1 \ldots M-1;\ j = i+1 \ldots M) \tag{51}$$

It should be noted that, if the ith and jth subdomain have no common boundary, $\boldsymbol{y}^{(i)}_{\partial\Omega_{ij}}$ is a zero-order vector and Eqs. (50) and (51) are no longer valid. The system of Eq. (48) and the interface continuity conditions,

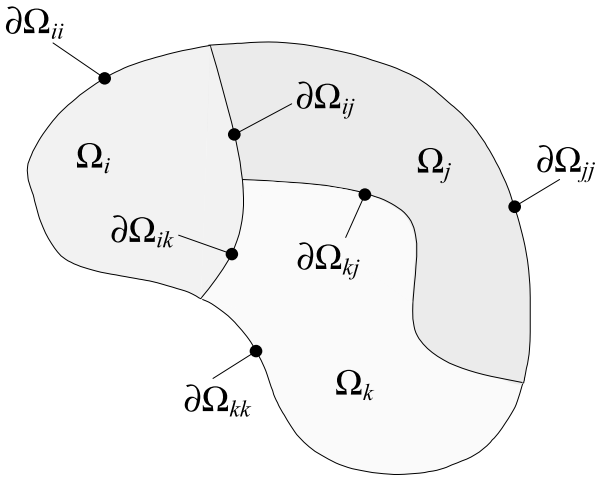

Fig. 1. Multidomain configuration.

Eqs. (50) and (51), provides a set of relationships, which, together with the external boundary conditions on the external boundaries $\partial\Omega_{ii}$ $(i = 1 \ldots M)$, allows one to obtain the electromechanical response in terms of extended displacement and traction on the boundary of each subdomain. The multidomain approach may be successfully used to model general fracture mechanics problems in homogeneous and inhomogeneous piezoelectric bodies (Aliabadi, 1997). The scheme is to introduce artificial interface boundaries, which connect the crack tips to the external boundary. By so doing the original cracked domain is divided into subregions whose boundaries contain the crack surfaces. Applying suitable boundary conditions on the crack surfaces (Dunn, 1994b), the multidomain boundary element approach provides the solution, which directly supplies the crack tip generalized tractions and displacements (Blandford et al., 1981). Indeed, these quantities coincide with the generalized tractions along the introduced artificial interface boundaries and the generalized displacements on the crack surfaces, respectively. Starting from these data it is possible to determine the generalized stress intensity factors (Suo et al., 1992) by using the well-established log-linear procedure (Raju and Crews, 1981; Davì and Milazzo, 1997) or the displacement correlation method (Blandford et al., 1981; Pan, 1999). A computer code has been developed to calculate the behavior of piezoelectric bodies by using the present approach. The computer code, called PZ-BEMD, implements the multidomain solution method and it is based on the following features. The influence coefficients are computed by Gaussian quadrature, assuming linear shape functions to express the generalized displacements and tractions on the boundary elements. An adaptive integration scheme has been applied which allows one to numerically take the kernel singularities into account (Davì, 1989). According to Eq. (28), the coefficients $\mathbf{c}^*$ are also computed by using Gaussian quadrature. The interface continuity conditions are enforced detecting automatically the boundaries common to contiguous subdomains by means of an interface identification algorithm, which implements the partition introduced in Eqs. (49), (50) and (51).

6. Applications and discussion

The piezoelectric material used in the computations is lead titanate–zirconate or PZT-4 ceramic whose material constants can be found in Table 1 (Berlincourt et al., 1964). The case of a finite crack of length $2a$ $(= 1$ m) in an infinite domain under uniform far-field stresses and normal electric displacement has been analyzed. This study was carried out to establish confidence and reliability in the method by comparing the present results with the exact solutions (Suo et al., 1992; Park and Sun, 1995). The infinite domain has been simulated by truncating it into a square with its dimension being 20 times the crack length (Tan et al., 1992). The analysis has been performed using 62 boundary elements for each of the two subdomains used in the modelization. First the capability of the approach to depict the crack tip singular behavior was investigated using the log-linear procedure (Davì and Milazzo, 1997), briefly described in the following. The generalized stress distribution along a radial line from the crack tip can be approximated by (Pak, 1992)

$$\Sigma_i \cong \left(K_i/\sqrt{2\pi}\right) r^{\alpha} \tag{52}$$

Table 1
Material constants of PZT-4

Elastic constants (N/m^2)	Piezoelectric constants (C/m^2)	Dielectric constants (C/Vm)
C_{11} 139×10^9		
C_{22} 115×10^9	e_{21} -5.2	ε_{11} 6.46×10^{-9}
C_{12} 74.3×10^9	e_{22} 15.1	
C_{13} 77.8×10^9	e_{14} 12.7	ε_{22} 5.62×10^{-9}
C_{44} 25.6×10^9		

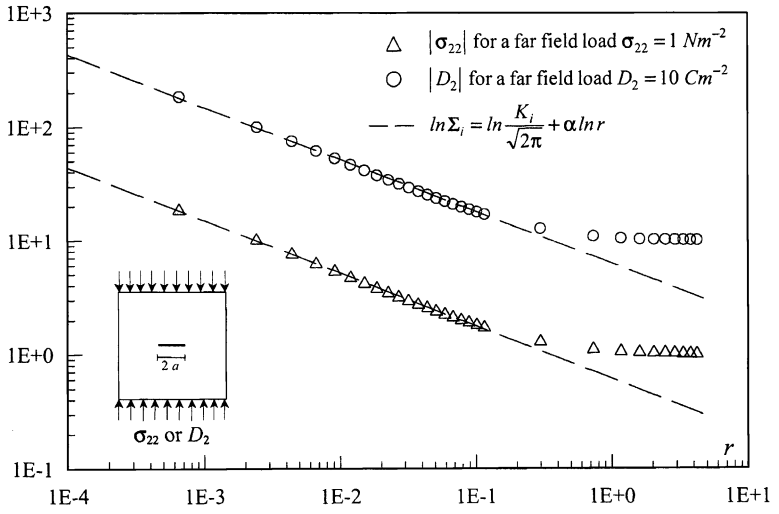

Fig. 2. Log-linear analysis for far-field constant loads.

where K is the generalized stress intensity factor, α is the crack tip singularity power and r is the distance from the crack tip. This equation is fitted to the stresses computed along a radial interface starting from the crack tip. If the equation fits well the numerical data, the singularity power and the generalized stress intensity factor can be determined from the slope and the Σ-intercept of the log Σ vs. log r plot. The stress patterns computed by the present method fit very well Eq. (52) near the crack tip. This is shown in Fig. 2 where the results obtained for representative generalized stress components are plotted for both mechanical and electric loads. Table 2 lists the generalized relative crack displacements, which are in good agreement with the exact values evidencing again the accuracy of the present approach. Notice that the value of $\Delta\varphi$ caused by a far-field stress σ_{22} is equal to that of Δu_2 caused by a far-field electric displacement D_2 as a direct outcome of the extended reciprocity theorem. The previous analysis confirms that the present method is able to adequately describe crack tip singular behavior. On this basis the generalized stress intensity factors may be also ascertained by extending the displacement correlation method to piezoelectric fracture mechanics. The generalized displacement correlation method is founded on the correlation of the computed

Table 2
Generalized relative crack displacements for a horizontal crack in an infinite domain

d (m)[a]	$\sigma_{22} = 1$ N/m^2				$D_2 = 1$ C/m^2			
	Δu_2 (10^{-10} m)		$\Delta\varphi$ (10^{-1} V)		$\Delta\varphi$ (10^{8} V)		Δu_2 (10^{-1} m)	
	Present	Exact	Present	Exact	Present	Exact	Present	Exact
0.475	0.177	0.177	0.221	0.221	0.881	0.882	0.221	0.221
0.408	0.174	0.174	0.217	0.217	0.867	0.868	0.217	0.217
0.342	0.168	0.168	0.210	0.210	0.837	0.838	0.210	0.210
0.275	0.158	0.158	0.197	0.197	0.788	0.789	0.197	0.197
0.208	0.144	0.144	0.179	0.179	0.716	0.717	0.179	0.179
0.142	0.123	0.124	0.153	0.154	0.614	0.616	0.153	0.154
0.075	0.092	0.093	0.115	0.116	0.463	0.465	0.115	0.116
0.008	0.031	0.032	0.039	0.040	0.157	0.160	0.039	0.040

[a] Distance behind the crack tip.

Table 3
Generalized stress intensity factors for a horizontal crack in an infinite domain

	$K_I/\sigma_{22}\sqrt{\pi a}$	$K_{II}/\sigma_{12}\sqrt{\pi a}$	$K_{III}/\sigma_{32}\sqrt{\pi a}$	$K_{IV}/D_2\sqrt{\pi a}$
Present[a]	1.0008	1.0025	1.0004	1.0001
Present[b]	0.9992	0.9989	0.9997	0.9994
Exact	1.0000	1.0000	1.0000	1.0000

[a] Computed by using the log-linear procedure.
[b] Computed by using the generalized displacement correlation method.

generalized relative crack displacements with their crack tip asymptotic expression, according to the following relation (Suo et al., 1992)

$$\Delta\mathbf{U}(d) = \sqrt{\frac{2d}{\pi}}\mathbf{Y}\mathbf{K} \tag{53}$$

where $\mathbf{K}$ is the vector of the generalized stress intensity factors, $\Delta\mathbf{U}$ is the vector of the generalized relative crack displacements, d is the distance behind the crack tip and $\mathbf{Y}$ is a material dependent matrix whose expression was given by Suo et al. (1992). The normalized generalized stress intensity factors, computed by using both the log-linear procedure and the generalized displacement correlation method, are given in Table 3 for different far-field loading conditions. In the table, the comparison with the exact solution is also presented. The computations carried out confirm some interesting features of the behavior of cracked piezoelectric infinite domains. The generalized stress intensity factors are uncoupled among them as a far-field stress causes stress intensity factors only, whereas a far-field electric displacement induces an electric displacement intensity factor only. The effect of the electromechanical coupling is thoroughly revealed in the generalized displacements, which are usually coupled as shown in Table 2 (Pan, 1999). Based on the good results obtained for cracks in infinite domains, the analysis has been extended to cracked finite piezoelectric solids. In the following results are presented for a rectangular piezoelectric solid with a central crack ($a = 0.1$ m) inclined $\vartheta = 45°$ with respect to the positive x_1 direction. The ratios of crack length to width and of height to width are $a/w = 0.2$ and $h/w = 2$, respectively (see Fig. 3). The analysis was performed for the specimen loaded by uniform tension and electric displacement applied in the x_2 direction. Tables 4 and 5 list the normalized generalized stress intensity factors for the two loading conditions considered. The results are given for both the electromechanical coupled and uncoupled ($e_{ij} = 0$) case and they are compared with those given by Pan (1999). In Table 4, D^* is a nominal electric displacement expressed in the unit of C/m^2 and with amplitude equal to that of σ_{22} expressed in N/m^2. Analogously in Table 5, σ^* is a nominal stress expressed in the unit of N/m^2 and with amplitude equal to that of D_2 expressed in C/m^2. The present results show that for cracks in finite, rectangular piezoelectric solids the generalized stress intensity factors are usually coupled. This topic is particularly important for electric loads, which may induce large mechanical stress intensity factors. Conversely, the electric displacement stress intensity factors due to mechanical loads are usually negligible. It is however confirmed that the generalized stress intensity factors associated directly with the load do not feel much the electromechanical coupling, which instead affects noticeably the generalized relative crack displacement. This can be observed in Tables 6 and 7, which list the generalized relative crack displacements for the cracked rectangular piezoelectric body under mechanical and electrical loads. Results are presented for both coupled and uncoupled case to highlight the electromechanical coupling between the displacements and electric potential, which may be a primary concern in the design of piezoelectric devices. Actually, a mechanical load induces both relative crack displacements and electric potential and, vice versa, an electric load gives rise to both relative crack displacements and electric potential.

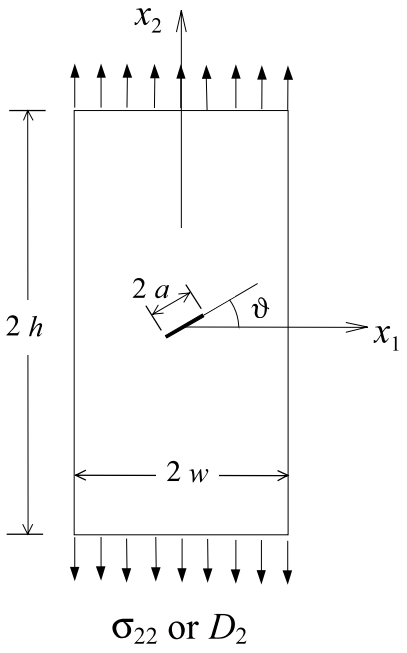

Fig. 3. Finite rectangular piezoelectric solid with an inclined crack.

Table 4
Generalized stress intensity factors for 45° inclined crack in a rectangular solid loaded by normal stress

		$K_I/\sigma_{22}\sqrt{\pi a}$	$K_{II}/\sigma_{22}\sqrt{\pi a}$	$K_{IV}/D^*\sqrt{\pi a}$
Coupled	Present	0.5292	0.5163	-2.79×10^{-12}
	Pan (1999)	0.5303	0.5151	-2.97×10^{-12}
Uncoupled	Present	0.5252	0.5154	0.0000
	Pan (1999)	0.5275	0.5151	0.0000

Table 5
Generalized stress intensity factors for 45° inclined crack in a rectangular solid loaded by electric displacement

		$K_I/\sigma^*\sqrt{\pi a}$	$K_{II}/\sigma^*\sqrt{\pi a}$	$K_{IV}/D_2\sqrt{\pi a}$
Coupled	Present	-1.44×10^6	1.64×10^5	−0.7283
	Pan (1999)	-1.42×10^6	1.69×10^5	−0.7278
Uncoupled	Present	0.0000	0.0000	−0.7256
	Pan (1999)	0.0000	0.0000	−0.7277

7. Conclusions

A boundary element formulation for the analysis of piezoelectric solids has been presented with the aim of exploiting its features in piezoelectric linear fracture mechanics. The electroelastic response of cracked piezoelectric solids has been determined by using a multidomain approach. This approach allows formulating the problem only in terms of the generalized displacement boundary integral equation, avoiding

Table 6
Generalized relative crack displacements for a 45° inclined crack in a rectangular solid loaded by $\sigma_{22} = 1$ N/m^2

$x_1 = x_2$ (10^{-1} m)	Coupled			Uncoupled	
	Δu_1 (10^{-13} m)	Δu_2 (10^{-11} m)	$\Delta\varphi$ (10^{-2} V)	Δu_1 (10^{-13} m)	Δu_2 (10^{-11} m)
0.477	0.256	−0.190	0.232	0.274	−0.271
0.424	0.279	−0.206	0.252	0.298	−0.295
0.371	0.299	−0.219	0.268	0.318	−0.313
0.318	0.315	−0.230	0.281	0.335	−0.329
0.265	0.328	−0.239	0.292	0.348	−0.341
0.212	0.339	−0.246	0.300	0.359	−0.352
0.159	0.347	−0.251	0.307	0.367	−0.359
0.106	0.352	−0.255	0.312	0.373	−0.365
0.053	0.356	−0.257	0.314	0.377	−0.368

Table 7
Generalized relative crack displacements for a 45° inclined crack in a rectangular solid loaded by $D_2 = 1$ C/m^2

$x_1 = x_2$ (10^{-1} m)	Coupled			Uncoupled
	Δu_1 (10^{-5} m)	Δu_2 (10^{-2} m)	$\Delta\varphi$ (10^{8} V)	$\Delta\varphi$ (10^{8} V)
0.477	0.353	0.232	0.093	0.175
0.424	0.371	0.252	0.100	0.189
0.371	0.385	0.268	0.107	0.201
0.318	0.391	0.281	0.112	0.211
0.265	0.406	0.292	0.116	0.219
0.212	0.410	0.300	0.120	0.226
0.159	0.416	0.307	0.123	0.230
0.106	0.420	0.312	0.125	0.234
0.053	0.431	0.314	0.126	0.236

hypersingular kernels. The solution of the model is achieved by BEM and the numerical results show the capability of the method to accurately assess the behavior of piezoelectric bodies without assumptions on the crack tip stress and electric states. On this basis, investigations have been performed to calculate the generalized stress intensity factors and generalized relative crack displacements so that to study in depth the effects of the electromechanical interaction on the structural behavior. It is pointed up that these coupling effects need to be adequately taken into account for a sound modelization of piezoelectric fracture mechanics. The insight into the effects of the electromechanical coupling on the generalized stresses and displacements is then a primary concern for a successful design of piezoelectric devices and structural members. Moreover, the present electromechanical analysis suggests that for piezoelectric materials the crack initiation and propagation criteria cannot be a simple extension of the elasticity criteria, based on single stress intensity factor. In conclusion, the BEM presented in this paper is a powerful and effective tool in the context of the linear electroelastic fracture mechanics, which is the core for the definition of ''effective'' quantities in the damage nonlinear modelization of piezoelectric materials.

References

Aliabadi, M.H., 1997. Boundary element formulations in fracture mechanics. Applied Mechanics Review 50 (2), 83–96.
Allik, H., Hughes, T.J.R., 1970. Finite element method for piezoelectric vibrations. International Journal for Numerical Methods in Engineering 2 (2), 151–157.

Banerjee, P.K., Butterfield, R., 1981. Boundary Element Methods in Engineering Science. McGraw-Hill, Maidenhead.
Barnett, D.M., Lothe, J., 1975. Dislocations and line charges in anisotropic piezoelectric insulators. Physics State Solid (b) 67, 105–111.
Benjeddou, A., 2000. Advances in piezoelectric finite element modeling of adaptive structural elements: a survey. Computers and Structures 76 (1–3), 347–363.
Benveniste, Y., 1992. The determination of the elastic and electric fields in piezoelectric inhomogeneity. Journal Applied Physics 72 (3), 1086–1095.
Berlincourt, D.A., Curran, D.R., Jaffe, H., 1964. Piezoelectric and piezomagnetic materials and their function in transducers. In: Mason W.P. (Ed.), Physical Acoustics, vol. 1, Academic, New York, pp. 169–270.
Blandford, G.E., Ingraffea, A.R., Ligget, J.A., 1981. Two-dimensional stress intensity factor computations using boundary element method. International Journal for Numerical Methods in Engineering 17 (3), 387–404.
Chen, T., Lin, F.Z., 1995. Boundary integral formulations for three-dimensional anisotropic piezoelectric solids. Computational Mechanics 15 (6), 485–496.
Crawley, E.F., Luis, J., 1987. Use of piezoelectric actuators as elements of intelligent structures. AIAA Journal 25 (10), 1373–1385.
Crawley, E.F., 1994. Intelligent structures for aerospace: a technology overview and assessment. AIAA Journal 32 (8), 1689–1699.
Davì, G., 1989. A general boundary integral formulation for the numerical solution of bending multilayer sandwich plates. In: Brebbia, C.A., Connor, J.J. (Eds.), Advances in Boundary Elements. Proceedings of the 11th International Conference on Boundary Element Methods. Computational Mechanics Publications, Southampton, pp. 25–35.
Davì, G., Milazzo, A., 1997. Boundary element solution for the free edge stresses in composite laminates. Journal of Applied Mechanics 64 (3), 877–884.
Davì, G., Milazzo, A., 2000. Piezoelectric materials fracture mechanics using the multidomain boundary element method. Proceedings of the IASS-IACM Fourth International Colloquium on Computation of Shell and Spatial Structures. Crete, edited on CD-ROM.
Dunn, M.L., 1994a. Electroelastic Green's functions for transversely isotropic piezoelectric media and their application to the solution of inclusion and inhomogeneity problems. International Journal Engineering Science 32 (1), 119–131.
Dunn, M.L., 1994b. The effects of crack face boundary conditions on the fracture mechanics of piezoelectric solids. Engineering Fracture Mechanics 48 (1), 25–39.
Hill, L.R., Farris, T.N., 1998. Three-dimensional piezoelectric boundary element method. AIAA Journal 36 (1), 102–108.
Kiral, E., Eringen, A.C., 1990. Constitutive Equations of Nonlinear Electromagnetic-Elastic crystals. Springer, Berlin.
Lee, J.S., Jiang, L.Z., 1994. A boundary integral formulation and 2D fundamental solution for piezoelectric media. Mechanical Research Communications 21 (1), 47–54.
Lee, J.S., 1995. Boundary element method for electroelastic interaction in piezoceramics. Engineering Analysis with Boundary Elements 15 (4), 321–328.
Lekhnitskii, S.G., 1963. Theory of Elasticity of an Anisotropic Body. Holden-Day, San Francisco.
Pak, Y.E., 1990a. Crack extension force in a piezoelectric material. Journal of Applied Mechanics 57 (3), 647–653.
Pak, Y.E., 1990b. Force on a piezoelectric screw dislocation. Journal of Applied Mechanics 57 (4), 863–869.
Pak, Y.E., 1992. Linear electro-elastic fracture mechanics of piezoelectric materials. International Journal of Fracture 54 (1), 79–100.
Pan, E., 1999. A BEM analysis of fracture mechanics in 2D anisotropic piezoelectric solids. Engineering Analysis with Boundary Elements 23 (1), 67–76.
Park, S.B., Sun, C.T., 1995. Effect of electric field on fracture of piezoelectric ceramics. International Journal of Fracture 70 (3), 203–216.
Parton, V.Z., 1976. Fracture mechanics of piezoelectric materials. Acta Astronautica 3 (9–10), 671–683.
Raju, I.S., Crews Jr, J.H., 1981. Interlaminar stress singularities at a straight free edge in composite laminate. Computers and Structures 14 (1–2), 21–28.
Sosa, H.A., Pak, Y.E., 1990. Three-dimensional eigenfunction analysis of a crack in a piezoelectric material. International Journal Solid Structures 26 (1), 1–15.
Sosa, H.A., Castro, M.A., 1990. On concentrated loads at the boundary of a piezoelectric half plane. Journal of Mechanics and Physics of Solids 42 (7), 1105–1122.
Suo, Z., Kuo, C.M., Barnett, D.M., Willis, J.R., 1992. Fracture mechanics for piezoelectric ceramics. Journal of Mechanics and Physics of Solids 40 (4), 739–765.
Tan, C.L., Gao, Y.L., Afagh, F.F., 1992. Boundary element analysis of interface cracks between dissimilar anisotropic materials. International Journal of Solids and Structures 29 (24), 3201–3220.
Wang, B., 1992. Three-dimensional analysis of an ellipsoidal inclusion in a piezoelectric material. International Journal Solids Structures 29 (3), 293–308.
Zhang, T.Y., Tong, P., 1996. Fracture mechanics for a mode III crack in a piezoelectric material. International Journal Solids Structures 33 (3), 343–359.
Zhong, Z., Meguid, S.A., 1997. Analysis of a circular arc-crack in piezoelectric materials. International Journal of Fracture 84 (2), 143–158.